International Journal of Power Electronics and Drive Systems (IJPEDS)
Vol. 14, No. 3, September 2023, pp. 1781~1790
ISSN: 2088-8694, DOI: 10.11591/ijpeds.v14.i3.pp1781-1790

Model predictive current control for maximum power point tracking of voltage source inverter based grid connected photovoltaic system

Satyanarayana Burada[1], Kottala Padma[2]
[1]Department of Electrical and Electronics Engineering, Anil Neerukonda Institute of Technology and Sciences (ANITS), Visakhapatnam, India
[2]Department of Electrical Engineering, Andhra University, Visakhapatnam, India

Article Info

Article history:

Received Jan 30, 2023
Revised Mar 28, 2023
Accepted Apr 6, 2023

Keywords:

3 phase inverters
Controller
Converter
Model predictive current control
MPPT
Photovoltaic system
Reference active current

ABSTRACT

Due to the high demand of grid connected photovoltaic systems, there is a need to track the maximum power point of the PV system. As the output of PV system is dc, there should be a converter, acting as medium between PV system and dc bus capacitor to track maximum power at all the loads. Usually boost converter is acting as medium between PV system and dc link capacitor as the duty cycle of the insulated-gate bipolar transistor in boost converter is in between 0 to 1 for maximum loads during maximum power point tracking (MPPT). To make PV system stable, the balance point is dc bus. If the dc bus voltage is constant, the system will be stable. Then the transfer power will just depend on current. For this purpose, the active current reference signal is to be generated by setting up the reference voltage across dc bus. Here to generate active reference current, PI controller is used and the reference voltage is taken according to the peak voltage of the inverter output voltage. The proposed control strategy was evaluated on a three-phase inverter linked to the grid and supplied by the PV system, which is working under varying irradiation conditions.

Corresponding Author:

Satyanarayana Burada
Department of Electrical and Electronics Engineering
Anil Neerukonda Institute of Technology and Sciences (ANITS)
Visakhapatnam, Andhra Pradesh, 531162, India
Email: satyanarayana.eee@anits.edu.in

1. INTRODUCTION

The decreasing of conventional power sources and reduction of PV cell cost have increased the using of photovoltaic systems. In photovoltaic (PV) systems maximum power point tracking (MPPT) methods becomes the part of control the power electronic converters [1]. Secondary control algorithms [1]–[5] are used to get better sensitivity and dynamic capability of control algorithms. Usually, renewable energy sources are used in microgrid where the group of loads are interconnected and clearly defined their electrical boundaries and acts as single controllable entity [6], [7] with respect to grid and can be connected in grid mode and islanded mode. for islanded networks there are some sensitivity-based methods to minimize the current during switching action [8], [9]. Usually sliding mode control (SMC) [10] and model predictive control (MPC) [2] algorithm is used to improve dynamic response. Even these techniques demand powerful computing, it has eliminated by technical improvements on micro controllers.

Different algorithms are proposed to track maximum power [11]–[13] from the PV systems at different loads. Adaptive neuro fuzzy inference and P&O MPPT algorithms are combined for better tracking of the maximum power [14]–[17]. It will give better results than the classical MPPT methods. Mechanical trackers are also used in tracking the maximum power from the PV system [18]–[20], but this is not a practical approach for high power rating PV systems. Advanced control algorithms are used to achieve a better dynamic reaction and sensitive control due to the challenges on the mechanical observer. The main advantage of sliding mode control is its fast dynamic response, robustness and insensitive to system parameters. But this work makes the argument that the model predictive control technique is used to produce the quick dynamic response. Model predictive control method is another method that has similar advantages as SMC. The MPPT algorithm is combined with MPC algorithm [21], [22] to obtain better maximum power tracking performance. Especially this combination gives good performance under variable irradiation conditions. This algorithm manages a Z-source inverter connected to the grid.

In this paper one stage power converter has been used. As two-stage power converters [21], [22] and [23], usage is increasing total cost of the system. But while using single stage power converter [24] series connected PV panel group is needed to get more dc bus voltage. Even there are different solutions to increase dc bus voltage [25]–[28] but one stage power layer with series PV panels is the most preferred model [24]–[29]. In this grid connected single stage power converter, the important parameter is the voltage across dc bus capacitor, which is to be maintained constant irrespective of the load for smooth and proper operation of the Z-source inverter. In this paper boost converter is used as the medium between PV system and dc bus capacitor as the firing angle of the power electronic switch is in between 0 to 1 for maximum loads during MPPT, which is not the case in buck type converter or buck boost converter. In this paper the comparison between buck, boost and buck-boost converter has been given for different load resistance values.

Here boost converter is used as the medium between PV system and dc bus capacitor and to boost up the input voltage of the inverter. To maintain the constant dc bus voltage the active current reference signal is to be generated by setting up the reference voltage across dc bus capacitor and as the reactive current is to be supplied by the grid, the reference reactive current is to be maintained at zero. Here to generate active reference current PI controller is used. And the reference voltage is taken according to the peak voltage of the inverter output voltage. The proposed control strategy was evaluated on a three-phase inverter linked to the grid and supplied by the PV system, which is working under varying irradiation and cloudy conditions.

Here one should think about some operational behavior of PI controller. That is according to irradiation curve, the PV irradiation will be zero for some time and after that it starts increasing. But during the zero-irradiation time, the generated power will be zero, so the converter cannot transfer any power to the dc bus, but the PI controller will work as usual and it will try to make dc bus voltage equal to reference voltage. It cannot be possible because generated power is zero and the PI controller will get saturated, when irradiation increases, the voltage starts increasing, but as already PI controller gets saturated power cannot transfer to the grid through inverter. So, the dc bus voltage reaches to very high value, so there is a need to reset PI controller by designing a reset condition. Here in this work, if the dc bus voltage is greater than 1.05 times that of reference voltage the PI controller will get reset. If there is no saturation point for the direct reference current, the reference current may increase to very higher value which may activate the over current relay and causes to nuisance tripping. So, a saturation point should be provided at the output of the PI controller.

2. SYSTEM MODEL AND OPERATION OF THE PROPOSED SYSTEM

2.1. Operation of the proposed system

Generally, in photo voltaic modules there is one single operating point at any given point in time where maximum power can be drawn, called as maximum power point. In this work MPPT algorithm is used to track the maximum power point of the photo voltaic system by controlling the duty cycle of the boost converter for different load conditions. The generated power from PV system is transferred to dc bus by boost converter and MPPT algorithm. The inverter transfers the power from dc bus to grid. The prediction algorithm is used to generate reference active component of current for inverter. The phase locked loop (PLL) is used to transform the three phase currents into dq0 transformation as the reference current signal is dc. By reducing the control parameter error between the standard and the subsequent sampling interval (Iabc(m+1)), the model predictive control algorithm operates. Model predictive control algorithm can be summarized in two steps as prediction and minimizing. To forecast the control value, discretization techniques are employed. The second stage of the model predictive control algorithm is error minimization. In the cost function and minimization block the PI controller is used to generate switching pulses to inverter through pulse width modulation technique, as shown in the simulation model.

2.2. Modelling of the proposed system

General circuit schema and controlling techniques are shown in Figure 1. PV system is directly connected to the grid through boost converter and 3 phase inverters. The values of filter inductance and capacitance can be calculated by (1) and (2), respectively [30].

$$L_{filter} = \frac{0.1u_{rms}^2}{2\pi f P_{phase}} \quad (1)$$

$$C_{filter} = \frac{0.05P_{phase}}{2\pi f u_{rms}^2} \quad (2)$$

Where u_{rms} is the line-to-line rms voltage from the grid side and P_{phase} is the single-phase power.

Here PV power is taken as a total system power for theoretical calculations. PV system consist 17 parallel strings and 14 series connected modules per each string and total input power is 50KW. The inductance and capacitance of the boost converter is calculated by (3) and (5), respectively [2].

$$L_{boost} = \frac{(1-D)^2.D.V_0^2}{2f_{sw}P} \quad (3)$$

Where D is the duty cycle, is the voltage across dc link capacitor, and f_{sw} is the switching frequency, P is the total power. The duty cycle can be calculated by using the (4).

$$D = 1 - \frac{V_{MPP}}{V_0} \quad (4)$$

Where V_{MPP} is the voltage of the PV system at maximum power point.

$$C_{boost} = \frac{D.P}{V_0^2.\%ripple.f_{sw}} \quad (5)$$

Here while designing capacitor value, percentage of ripple content to be taken as low as possible, but keep in the mind the cost of the capacitor banks. The maximum power point tracking (MPPT) is used to track maximum energy from PV panels at different irradiance levels. In any MPPT algorithm the duty cycle of the converter is changed to make the load resistance is equal to internal resistance of PV module to transfer maximum power from source to load. The comparison between buck, boost and buck-boost converter is shown in Table 1, in which it was observed that for 90% of the loads the duty cycle value of the boost converter is in between 0 and 1 and the continuous current can be drawn from the PV system due to the input inductance of the boost converter.

The reference current for the inverter is determined using the conventional P&O MPPT algorithm described in [2]. As a result, the model predictive current control approach is the main emphasis of this study, which is utilized to control inverter current (i_{abc}). The general voltage equation for the inverter [31] is given in (6). Here $V_{inverter}$ is the inverter voltage, V_{Lf} is the voltage drop due to filter inductance, V_{Rf} is the voltage drop due to filter resistance and V_{GRID} is the measured grid voltage.

$$V_{inverter} = V_{Lf} + V_{Rf} + V_{GRID} \quad (6)$$

Output current equation can be written by replacing of inductor voltages [31] in (7). Here $i_{(m)}$ is the current sample interval's inverter current, L_f is the filter inductance, $V_{inverter(l)}$ is the inverter voltage vector, $V_{GRID(m)}$ is the current sample interval's measured grid voltage and R_{Lf} is the filter resistance.

$$\frac{di_{(m)}}{dt} = \frac{1}{L_f}(V_{inverter(l)} - V_{GRID(m)} - R_{Lf}i_{(m)}) \quad (7)$$

Where $V_{GRID(m)}$ is the current sample interval's measured grid voltage. All measured parameters are converted using the Clarke transformation into α-β coordinate. $V_{inverter}$ stands for inverter voltage vector, which is used to make predictions. The voltage space vectors are given in Figure 2. There are two "0" states and six active states in three-phase inverters, as shown in the diagram. It demonstrates that there are eight states in which the inverter can function. An array of phase states represents all voltage states (S_A, S_B, S_C). In (8) – α-β frame [28] can be used to express inverter voltage states. As a result, all of the control parameters in (7) are in the α-β frame.

$$V_{inverter(l)} = \frac{2}{3}\left[S_{A(l)} + (-0.5 + 0.866j)S_{B(l)} + (-0.5 - 0.866j)S_{C(l)}\right] \quad (8)$$

In the (8), l is state number that varies from {1,2……………8}.

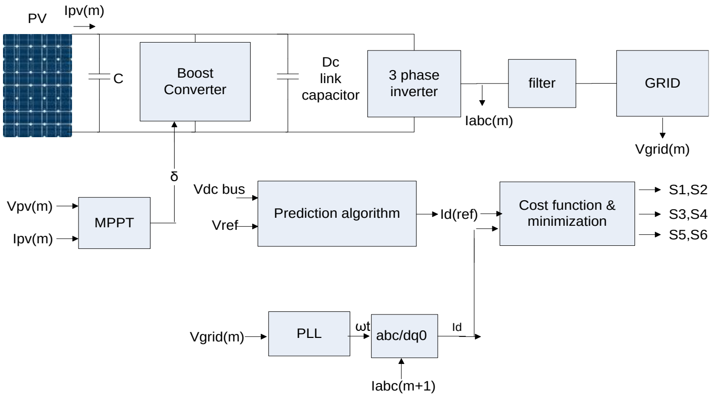

Figure 1. General schematic diagram of the system

Table 1. Duty cycle of buck, boost and buck-boost converter for different loads

R_0 (Ω)	δ (boost)	δ (buck)	δ (buck boost)	R_0 (Ω)	δ (boost)	δ (buck)	δ (buck boost)
2	-0.95157	0.51241	0.3388	52	0.61727	2.6128	0.7232
4	-0.37997	0.72465	0.42017	54	0.62442	2.6626	0.72697
6	-0.12674	0.88752	0.4702	56	0.63119	2.7114	0.73056
8	0.024216	1.0248	0.50613	58	0.6376	2.7594	0.734
10	0.12723	1.1458	0.53397	60	0.64369	2.8066	0.7373
12	0.20328	1.2551	0.55657	62	0.64949	2.853	0.74046
14	0.26238	1.3557	0.5755	64	0.65501	2.8986	0.7435
16	0.31002	1.4493	0.59172	66	0.66028	2.9436	0.74642
18	0.34948	1.5372	0.60587	68	0.66531	2.9878	0.74924
20	0.38286	1.6204	0.61838	70	0.67012	3.0314	0.75195
22	0.41158	1.6995	0.62956	72	0.67474	3.0744	0.75457
24	0.43663	1.775	0.63964	74	0.67916	3.1169	0.7571
26	0.45873	1.8475	0.64882	76	0.68341	3.1587	0.75954
28	0.47842	1.9173	0.65721	78	0.6875	3.2000	0.7619
30	0.49511	1.9845	0.66494	80	0.69143	3.2408	0.76419
32	0.51211	2.0496	0.67209	82	0.69522	3.281	0.76641
34	0.52668	2.1127	0.67874	84	0.69887	3.3208	0.76856
36	0.54001	2.174	0.68494	86	0.70239	3.3601	0.77065
38	0.55228	2.2335	0.69074	88	0.70579	3.3989	0.77267
40	0.56362	2.2916	0.69619	90	0.70908	3.4373	0.77464
42	0.57413	2.3481	0.70133	92	0.71226	3.4753	0.77655
44	0.58392	2.4034	0.70618	94	0.71533	3.5129	0.77841
46	0.59307	2.4574	0.71077	96	0.71832	3.5501	0.78022
48	0.60164	2.5103	0.71512	100	0.72401	3.6233	0.7837
50	0.60969	2.562	0.71926				

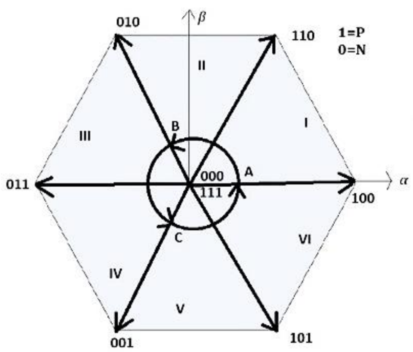

Figure 2. Space vectors of three-phase two level inverter

3. METHOD FOR MODELING PREDICTIVE CURRENT CONTROL

Between the reference and the next sample period, the MPC algorithm minimizes the control parameter error. MPC consists of two phases. prediction and minimization. Discrete method discretization is employed to anticipate the control parameter. Usually, exact discretization method has high accuracy for low order and high order systems but it will take a greater number of iterations and more computational time. The forward Euler approximation method also has high accuracy for low order systems with a smaller number of iterations and less computational time. The local truncation error or local discretization error in the Euler method is the error made in approximating the derivative by the difference quotient, whereas the global discretization error at a position is the magnitude of the actual error at the point. so, (9) is a first order differential equation. So, the forward Euler approximation [31] method is preferred.

$$\frac{di}{dt} \approx \frac{i_{(m+1)} - i_{(m)}}{T_s} \tag{9}$$

In (10) can be produced by replacing the derivative in (7) with the Euler technique.

$$\frac{i_{(m+1)} - i_{(m)}}{T_s} = \frac{1}{L_f}\left(V_{inverter} - V_{GRID(m)} - R_{Lf}\, i_{(m)}\right) \tag{10}$$

You may get the prediction in (11) by arranging the (10).

$$i_{(m+1)} = \left[\frac{T_s}{L_f}\left(V_{inverter(l)} - V_{GRID(m)} - R_{Lf}\, i_{(m)}\right)\right] + i_{(m)} \tag{11}$$

In (11) predicts current values for all possible voltage states (1....n). Error minimization is the second stage of the MPC method, as was already mentioned. Most control methods use the difference between the reference and measured values. Unlike previous approaches, Utilizing the discrepancy between the reference and predicted values, the MPC algorithm. This feature allows the algorithm to create an action for the subsequent phase. As a result, MPC has a greater dynamic range. In MPC algorithms, in order to calculate the error term, cost functions are used. The control algorithm's cost function is represented by (12). Real and imaginary current values are denoted by i_α and i_β respectively.

$$g = \left|i_\alpha^* - i_{\alpha(m+1)}\right| + \left|i_\beta^* - i_{\beta(m+1)}\right| \tag{12}$$

For each sample interval, the cost function is evaluated along with the prediction equation for all potential voltage vectors. As a result, error values are generated for every possible switching position. The best cost function with the least amount of error is selected during the minimization stage. In order to create switching signals, the optimum cost function is used.

4. SIMULATION RESULTS

Simulation studies are used to verify the system model and proposed control structures in Figure 1. Table 2 lists the simulation parameters. Firstly, the proposed control algorithm's power flow control performance has been tested under various irradiation conditions. The simulation model is shown in Figures 3(a)-(c).

Table 2. System specifications

Parameter	Value
u_{rms}(Grid voltage)	380 V
f (Grid frequency)	50 Hz
P (Nominal power)	50.72 kW
L_{Filter} (Filter inductance per phase)	0.0028 H
L_{boost} (Inductance of boost converter)	1.6236 mH
C (DC link capacitor)	1000 µF
PV Panel (17 parallel and 14 series)	50.72 kW_{MPP},406 V_{MPP}
T_s(Sampling time)	10 µs

Following the dynamic performance analysis, the suggested control algorithm's power flow control performance was tested under various irradiation situations. Figure 4 shows the irradiation curve during the course of 30 seconds [11]. This paper presents a method that overcomes the problem of the confusion during fast irradiation change in the classical MPPT as well as in model predictive control (MPC) based MPPTs available in the literature.

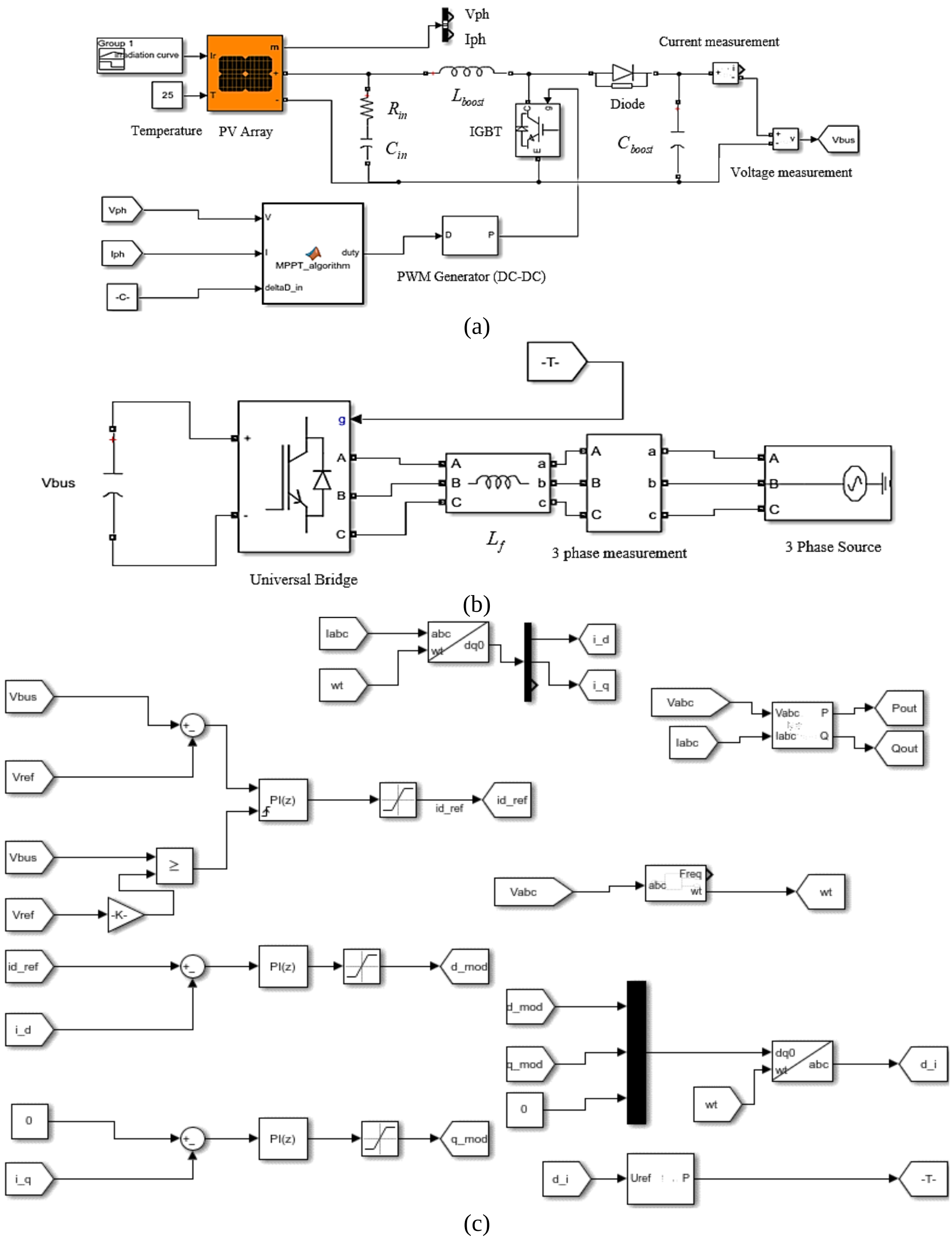

Figure 3. Simulation models for grid connected PV system: (a) DC side of the system, (b) AC side of the system, and (c) reference active current generation and control unit

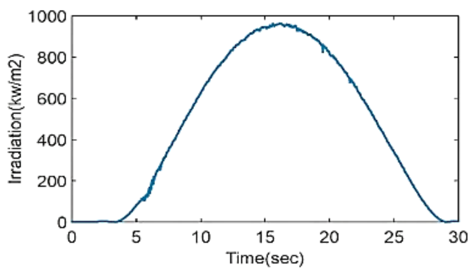

Figure 4. Irradiation curve

Figure 5 shows the PV power results. The MPPT algorithm tracks the MPP with 98 percent efficiency, as shown in Figures 5(a) and 5(b). Even though efficiency decreased in cloudy conditions, after these times, efficiency increased to 98 percent. Figures 5(c) and 5(d) show the voltage and current results for the PV panel group, respectively. While the current rises to 125 A, The PV voltage is fairly stable. It results from the nature of MPPT control in PVs and offers information on control effectiveness. The reference voltage for the PI controller to generate direct component of reference current, should be selected based on the voltage across dc bus capacitor, when it is disconnected from the PV system and charged by the inverter. As the inverter is mostly buck type inverter, The dc bus voltage needs to be higher than the inverter output voltage's maximum value.

Here one should concentrate on some operational behavior of PI controller. That is according to irradiation curve, the PV irradiation will be zero for some time and after that it starts increasing. But during the zero-irradiation time, the generated power will be zero, so the converter cannot transfer any power to the dc bus, but the PI controller will work as usual and it will try to make dc bus voltage equal to reference voltage. It cannot be possible because generated power is zero and the PI controller will get saturated, when irradiation increases, the voltage starts increasing, but as already PI controller gets saturated power cannot transfer to the grid through inverter. So, the dc bus voltage reaches to very high value, so there is a need to reset PI controller by designing a reset condition.

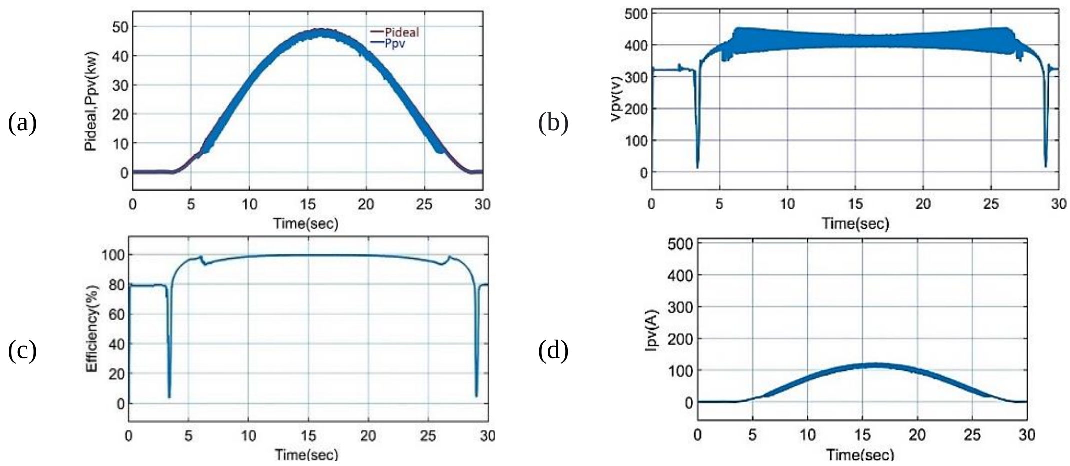

Figure 5. PV results: (a) power, (b) MPPT efficiency, (c) PV voltage, and (d) PV current

Here in this work, if the dc bus voltage is greater than 1.05 times that of reference voltage the PI controller will get reset. If there is no saturation point for the direct reference current, the reference current may increase to very higher value which may activate the over current relay and causes to nuisance tripping. So, a saturation point should be provided at the output of the PI controller to limit the current with in specified range. Figure 6 shows the reference voltage that must be selected for proper operation of PI controller to generate active component of reference current. The active reference current will be generated based on the difference between dc bus voltage and reference voltage. The active component of the reference current is shown in Figure 7. And the voltage across the capacitor, which is also called as dc bus voltage is maintained constant, irrespective of the load and for the given system it is maintained at 800 V as shown in Figure 8.

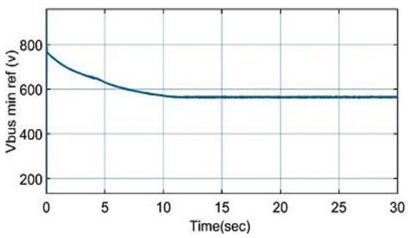

Figure 6. Reference voltage for dc bus voltage

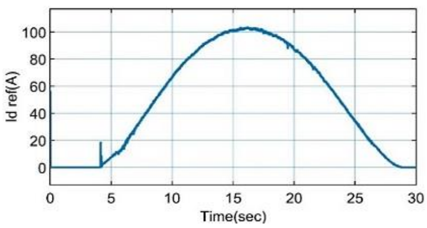

Figure 7. Reference current for the PI controller

Aside from the MPPT algorithm's performance, one must examine the power, effectiveness, and harmonic distortions of the inverter side. The MPC method correctly fixes the inverter currents to the reference value (Iref*) as illustrated in Figure 9(a). The inverter's output currents are also altered in accordance with the irradiation curve in Figure 4. Because The reference current value is adjusted by the MPPT algorithm and MPC. Harmonics are less than 5% for active power values greater than 20 kW, as shown in Figure 9(b). The THD value is less than the limit set forth in the standards [32].

Here the PI controller will trigger the inverter to make the peak current of the inverter output equal to the active component of the reference current as shown in Figure 10. Detailed results of inverter currents shown in Figure 11(a). The MPC algorithm successfully regulates the inverter currents to the reference. According to recent tracking data, the combined control algorithms reliably follow the MPP under hazy and variable irradiance conditions. Detailed results of the inverter voltages are shown in Figure 11(b). The inverter voltages are successfully synchronized with the grid voltage of line-to-line RMS value of 380 V. Irrespective of the load the MPC algorithm always keep the inverter voltage equals to the grid voltage.

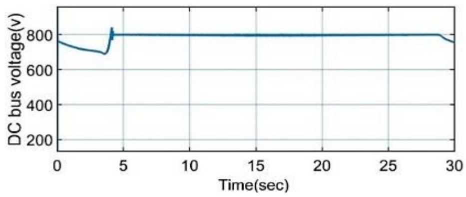

Figure 8. DC bus voltage

(a)

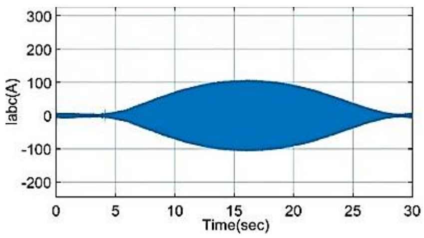

(b)

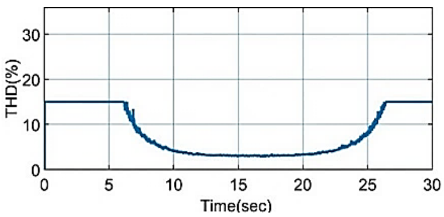

Figure 9. Inverter results: (a) currents and (b) THD

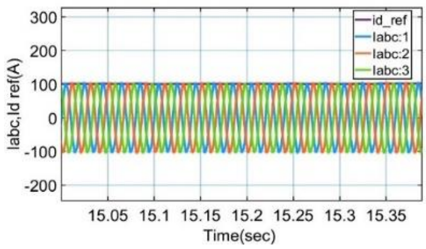

Figure 10. Line currents of the inverter and reference active current

(a)

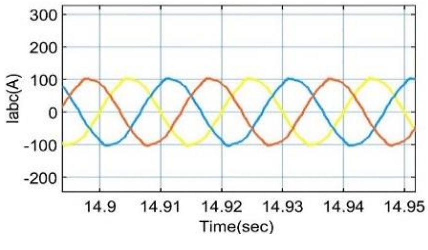

(b)

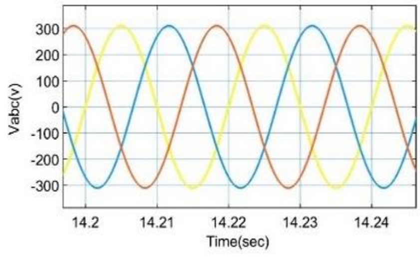

Figure 11. Detailed inverter results: (a) line currents and (b) line voltages

To evaluate the total efficiency of the proposed system, the transferred power to grid at the output of the inverter was compared to ideal MPP curves. Figure 12 depicts the power losses between the inverter output power and the desired maximum power curve. Around the nominal power, power losses are quite high. Filter inductance is to blame. The losses in a practical inductor come mainly from the parasitic equivalent resistance (which is practically the ohmic resistance of the windings which depends on the geometry of the wire used in winding the inductor as well as the frequency) and the core losses. To reduce the major losses in the filter inductor the toroidal shape inductor is used. Due to its symmetry, the toroidal shape has the benefit of having a low leakage flux, or the quantity of magnetic flux that escapes the core is low, therefore the core losses will be less and by keeping the ohmic resistance of the inductor low the copper losses can be reduced. Even if losses increased, figure demonstrates that for power values more than 5 kW, the minimum system efficiency is around 90%.

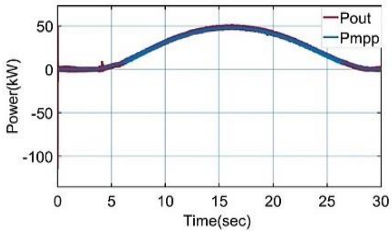

Figure 12. Inverter output power and ideal MPP curve

5. CONCLUSION

A combined control algorithm for PV systems is suggested in the paper. The MPPT and MPC algorithms are used in the suggested control strategy. The integrated algorithm provided efficient tracking under variable irradiance and foggy situations because of the quick and sensitive control capabilities of MPC. In addition to the combined algorithm performance testing, the step-change tests demonstrate that the MPC algorithm has a superior capability for current control. It has been done to analyze the efficiency of both control and power structures. The MPPT method's control efficiency is 98 percent, while the inverter efficiency is 92 percent. Both the inverter and the control algorithms overall system efficiency are around 90%.

REFERENCES

[1] M. Metry, M. B. Shadmand, R. S. Balog, and H. Abu-Rub, “MPPT of photovoltaic systems using sensorless current-based model predictive control,” *IEEE Transactions on Industry Applications*, vol. 53, no. 2, pp. 1157–1167, 2017, doi: 10.1109/TIA.2016.2623283.

[2] E. Irmak and N. Güler, “A model predictive control-based hybrid MPPT method for boost converters,” *International Journal of Electronics*, vol. 107, no. 1, pp. 1–16, 2020, doi: 10.1080/00207217.2019.1582715.

[3] E. Kabalci, G. Gokkus, and A. Gorgun, “Design and implementation of a PI-MPPT based buck-boost converter,” *Proceedings of the 2015 7th International Conference on Electronics, Computers and Artificial Intelligence, ECAI 2015*, pp. SG23–SG28, 2015, doi: 10.1109/ECAI.2015.7301194.

[4] I. Chtouki, P. Wira, M. Zazi, B. Collicchio, and S. Meddour, “Design, implementation and comparison of several neural Perturb and Observe MPPT methods for photovoltaic systems,” *International Journal of Renewable Energy Research*, vol. 9, no. 2, pp. 757–770, 2019, doi: 10.20508/ijrer.v9i2.9293.g7645.

[5] N. Genc, H. Uzmus, and I. Iskender, “Dynamic behavior of DC-DC boost converter controlled with cascade PI-ASC,” *Proceedings of the 8th International Conference on Electronics, Computers and Artificial Intelligence, ECAI 2016*, 2017, doi: 10.1109/ECAI.2016.7861148.

[6] E. Loukakis and E. Karapidakis, “Feasibility study of microgrid village with renewable energy sources,” *2017 52nd International Universities Power Engineering Conference, UPEC 2017*, vol. 2017-January, pp. 1–6, 2017, doi: 10.1109/UPEC.2017.8231889.

[7] A. Paspatis, K. Fiorentzis, Y. Katsigiannis, and E. Karapidakis, “Smart campus microgrids towards a sustainable energy transition—the case study of the Hellenic Mediterranean University in Crete,” *Mathematics*, vol. 10, no. 7, 2022, doi: 10.3390/math10071065.

[8] E. E. Pompodakis, G. C. Kryonidis, M. C. Alexiadis, and E. S. Karapidakis, “A Three-phase sensitivity-based approach for smooth line-switching in islanded networks,” *International Journal of Electrical Power and Energy Systems*, vol. 144, 2023, doi: 10.1016/j.ijepes.2022.108515.

[9] E. E. Pompodakis, G. C. Kryonidis, and E. S. Karapidakis, “Volt/Var control and energy management in Non-Interconnected insular networks with multiple hybrid power plants,” *Applied Energy*, vol. 331, 2023, doi: 10.1016/j.apenergy.2022.120427.

[10] K. Amara *et al.*, “Improved performance of a PV solar panel with adaptive neuro fuzzy inference system ANFIS based MPPT,” *7th International IEEE Conference on Renewable Energy Research and Applications, ICRERA 2018*, pp. 1098–1101, 2018, doi: 10.1109/ICRERA.2018.8566818.

[11] A. A. Abdulrazzaq and A. H. Ali, “Efficiency performances of two MPPT algorithms for PV system with different solar panels irradiances,” *International Journal of Power Electronics and Drive Systems*, vol. 9, no. 4, pp. 1755–1764, 2018, doi: 10.11591/ijpeds.v9.i4.pp1755-1764.

[12] N. Hashim, Z. Salam, D. Johari, and N. F. N. Ismail, “DC-DC boost converter design for fast and accurate MPPT algorithms in stand-alone photovoltaic system,” *International Journal of Power Electronics and Drive Systems*, vol. 9, no. 3, pp. 1038–1050, 2018, doi: 10.11591/ijpeds.v9.i3.pp1038-1050.

[13] T. Laagoubi, M. Bouzi, and M. Benchagra, “MPPT and power factor control for grid connected PV systems with fuzzy logic controllers,” *International Journal of Power Electronics and Drive Systems (IJPEDS)*, vol. 9, no. 1, p. 105, Mar. 2018, doi: 10.11591/ijpeds.v9.i1.pp105-113.

[14] S. Biricik, H. Komurcugil, N. D. Tuyen, and M. Basu, “Protection of sensitive loads using sliding mode controlled three-phase DVR with adaptive notch filter,” *IEEE Transactions on Industrial Electronics*, vol. 66, no. 7, pp. 5465–5475, 2019, doi: 10.1109/TIE.2018.2868303.

[15] D. Haji and N. Genc, “Fuzzy and P&O Based MPPT controllers under different conditions,” in *2018 7th International Conference on Renewable Energy Research and Applications (ICRERA)*, Oct. 2018, pp. 649–655. doi: 10.1109/ICRERA.2018.8566943.

[16] N. Priyadarshi, A. K. Sharma, and F. Azam, “A hybrid firefly-asymmetrical fuzzy logic controller based MPPT for PV -wind-fuel grid integration,” *International Journal of Renewable Energy Research*, vol. 7, no. 4, pp. 1546–1560, 2017, doi: 10.20508/ijrer.v7i4.6131.g7195.

[17] M. Heidari, “Improving efficiency of photovoltaic system by using neural network MPPT and predictive control of converter,” *International Journal of Renewable Energy Research*, vol. 6, no. 4, pp. 1524–1529, 2016, doi: 10.20508/ijrer.v6i4.4794.g6942.

[18] A. Fudholi, L. C. Haw, K. Sopian, and A. M. Omer Abdulmula, “Primary study of tracking photovoltaic system for mobile station in Malaysia,” *International Journal of Power Electronics and Drive Systems (IJPEDS)*, vol. 9, no. 1, p. 427, Mar. 2018, doi: 10.11591/ijpeds.v9.i1.pp427-432.

[19] A. A. Sneineh and W. A. Salah, “Design and implementation of an automatically aligned solar tracking system,” *International Journal of Power Electronics and Drive Systems*, vol. 10, no. 4, pp. 2055–2064, 2019, doi: 10.11591/ijpeds.v10.i4.pp2055-2064.

[20] S. H. Chong, N. N. Chandren, and C. R. Allan Soon, “Output energy maximization of a single axis photovoltaic solar tracking system: Experimental verification,” *International Journal of Power Electronics and Drive Systems*, vol. 10, no. 3, pp. 1655–1661, 2019, doi: 10.11591/ijpeds.v10.i3.pp1655-1661.

[21] N. Altin, S. Ozdemir, H. Komurcugil, I. Sefa, and S. Biricik, “Two-stage grid-connected inverter for PV systems,” *Proceedings - 2018 IEEE 12th International Conference on Compatibility, Power Electronics and Power Engineering, CPE-POWERENG 2018*, pp. 1–6, 2018, doi: 10.1109/CPE.2018.8372540.

[22] M. B. Shadmand, X. Li, R. S. Balog, and H. A. Rub, “Model predictive control of grid-tied photovoltaic systems: Maximum power point tracking and decoupled power control,” *2015 1st Workshop on Smart Grid and Renewable Energy, SGRE 2015*, 2015, doi: 10.1109/SGRE.2015.7208726.

[23] I. Colak, E. Kabalci, and G. Bal, “Parallel DC-AC conversion system based on separate solar farms with MPPT control,” *8th International Conference on Power Electronics - ECCE Asia: “Green World with Power Electronics”, ICPE 2011-ECCE Asia*, pp. 1469–1475, 2011, doi: 10.1109/ICPE.2011.5944473.

[24] S. Ozdemir, N. Altin, and I. Sefa, “Single stage three level grid interactive MPPT inverter for PV systems,” *Energy Conversion and Management*, vol. 80, pp. 561–572, 2014, doi: 10.1016/j.enconman.2014.01.048.

[25] S. Sajadian, R. Ahmadi, and H. Zargarzadeh, “Extremum seeking-based model predictive MPPT for grid-tied z-source inverter for photovoltaic systems,” *IEEE Journal of Emerging and Selected Topics in Power Electronics*, vol. 7, no. 1, pp. 216–227, 2019, doi: 10.1109/JESTPE.2018.2867585.

[26] M. Kamalirad, H. Iman-Eini, B. Farhangi, and S. Bacha, “A reliable three-phase transformerless grid-connected PV inverter with inductive DC link,” *IEEE Journal of Photovoltaics*, vol. 8, no. 5, pp. 1305–1312, 2018, doi: 10.1109/JPHOTOV.2018.2846702.

[27] N. Genc and Y. Koc, “Experimental verification of an improved soft-switching cascade boost converter,” *Electric Power Systems Research*, vol. 149, pp. 1–9, 2017, doi: 10.1016/j.epsr.2017.04.015.

[28] E. Irmak and N. Guler, “Model predictive control of grid-tied three level neutral point clamped inverter integrated with a double layer multi-input single output DC/DC converter,” *Proceedings - 2018 IEEE 12th International Conference on Compatibility, Power Electronics and Power Engineering, CPE-POWERENG 2018*, pp. 1–6, 2018, doi: 10.1109/CPE.2018.8372538.

[29] A. Sangwongwanich and F. Blaabjerg, “Mitigation of interharmonics in PV systems with maximum power point tracking modification,” *IEEE Transactions on Power Electronics*, vol. 34, no. 9, pp. 8279–8282, 2019, doi: 10.1109/TPEL.2019.2902880.

[30] M. W. Hussain and M. A. Qureshi, “Analysis and design of passive filters for power quality improvement in 3φ grid-tied PV systems,” *2021 4th International Conference on Energy Conservation and Efficiency, ICECE 2021 - Proceedings*, 2021, doi: 10.1109/ICECE51984.2021.9406278.

[31] A. Lashab, D. Sera, and J. M. Guerrero, “A dual-discrete model predictive control-based MPPT for PV systems,” *IEEE Transactions on Power Electronics*, vol. 34, no. 10, pp. 9686–9697, 2019, doi: 10.1109/TPEL.2019.2892809.

[32] IEEE Power and Energy Society (Transmission and Distribution Committee), “IEEE Recommended Practice and Requirements for Harmonic Control in Electric Power Systems,” *IEEE Std 519-2014*, vol. 2014, 2014.

BIOGRAPHIES OF AUTHORS

Satyanarayana Burada received B. Tech degree in Electrical and Electronics Engineering from JNTU Kakinada, India in 2012, M. Tech degree in Power Systems from National Institute of Technology (NIT), Surat, India in 2016 and currently pursuing PhD in grid connected photo-voltaic systems area from Andhra University, Visakhapatnam, India. He presented papers in 2 IEEE conferences held at Delhi Technological university in 2016 and Amity University in 2017. From 2016 until now he has been a lecturer in the department of Electrical and Electronics Engineering, Anil Neerukonda Institute of Technology and Sciences, Visakhapatnam, India. He can be contacted at email: satyanarayana.eee@anits.edu.in.

Kottala Padma has done her B. Tech from Sri Venkateswara University in 2005, MTech in Power Systems from Andhra University in 2010 and PhD from Andhra University in 2015. Presently working as Associate Professor of Electrical Engineering Department at Andhra University, Visakhapatnam, India. She has published 10 papers in SCI, Scopus, Web of Science indexed journals and 2 papers in springer book chapters. Her research interests include Power system aspects, Renewable energy systems, Microgrids, Internet of things, soft computing techniques, Transmission and Distribution systems. She has guided 2 Ph.D. Students and currently guiding 8 Research Scholars and has successfully supervised 30 PG thesis. She has been presented with Global Teacher Award and best research award. She can be contacted at email: dr.kpadma@andhrauniversity.edu.in.